Structure of the Gulf Stream and Its Recirculations at 55°W*

AMY S. BOWER AND NELSON G. HOGG

Woods Hole Oceanographic Institution, Woods Hole, Massachusetts

(Manuscript received 19 September 1994, in final form 18 October 1995)

ABSTRACT

Two years of direct current and temperature observations from an array of 13 current meter moorings deployed near 55°W as part of the SYNOP (Synoptic Ocean Prediction) Experiment have been used to explore the spatial and temporal variability of the Gulf Stream from three points of view. In the geographic reference frame, mean eastward velocities were observed from the surface to 4000 m. There was no evidence of westward flow south of the eastward jet, suggesting that the Worthington recirculation gyre was located south of the array during this time period. Westward flow was observed north of the jet only at 4000 m, where it had a magnitude comparable to the mean Gulf Stream (5–10 cm s^{-1}). These data also indicate that the mean eastward jet is much more vertically aligned than was depicted in an earlier picture constructed from noncontemporaneous observations. In the Lagrangian, or streamwise, reference frame, it was found that, at the thermocline level, the width of the "average synoptic" Gulf Stream and the velocity structure remain virtually unchanged between Cape Hatteras (73°W) and 55°W, in spite of large amplitude meandering. The barotropic velocity component of the average synoptic stream increases fivefold over this distance, and the baroclinic component weakens. The northern recirculation appears more clearly in the stream coordinate frame as a 130-km wide barotropic flow with peak westward velocities of about 8 cm s^{-1}. South of the stream, there was no evidence of westward flow, even in the stream coordinate system. Finally, a consideration of eddy–mean flow interactions in terms of the eddy energy equations shows that at the thermocline level, there were no significant cross-gradient fluxes of heat or momentum, supporting the notion that 55°W is at a maximum in eddy energy. At 4000 m, there was some indication of upgradient heat and momentum fluxes in the Gulf Stream, consistent with decreasing eddy energy following the mean flow to the east. These results point to the region between 55°W and the Tail of the Grand Banks (50°W) as the site of eddy energy decay in the Gulf Stream system.

1. Introduction

In the three decades that have passed since Stommel's comprehensive review of the Gulf Stream in 1965, our description of the basic structure of this energetic current has been significantly refined. This is due in large part to the many new observations that have been made with increasingly sophisticated instrumentation. But these observations have also revealed the complexities of the Gulf Stream's spatial and temporal variability, especially in the region between Cape Hatteras and the Grand Banks of Newfoundland. This is where meanders in the Gulf Stream's path grow to large amplitude, often pinching off to form warm and cold core rings. These meanders represent the major source of variability in the western North Atlantic (Halkin and Rossby 1985; Kelly 1991) and are probably responsible, at least in part, for the dissipation of potential vorticity gained in the wind-driven interior (Holland and Rhines 1980; Lozier and Riser 1990).

In the late 1980s, a large, multi-institutional program was undertaken to further improve our description of the Gulf Stream and, ultimately, our understanding of the dynamics controlling its variability. This effort, called SYNOP (Synoptic Ocean Prediction), consisted of theoretical, numerical, and observational studies of the Gulf Stream and its recirculations east of Cape Hatteras. As part of the observational component, four moored current meter arrays were maintained for two years: one near the separation point at Cape Hatteras (the Inlet Array), one upstream of the New England Seamount Chain (NESC) near 68°W (the Central Array), a third downstream of the NESC near 55°W (the Eastern Array), and the fourth at the Tail of the Grand Banks (the 50°W Array) (Fig. 1). In this work, we have analyzed the data from the Eastern Array to produce a comprehensive description of the velocity and temperature structure of the Gulf Stream and its recirculations near 55°W. These results are then compared to descriptions of the Gulf Stream at upstream locations in order to examine changes in Gulf Stream structure. This paper can be considered to be a companion to Hogg (1992), which used the Eastern Array data and direct velocity observations from three upstream loca-

* WHOI Contribution Number 8825.

Corresponding author address: Dr. Amy S. Bower, Department of Physical Oceanography, Woods Hole Oceanographic Institution, Woods Hole, MA 02543.

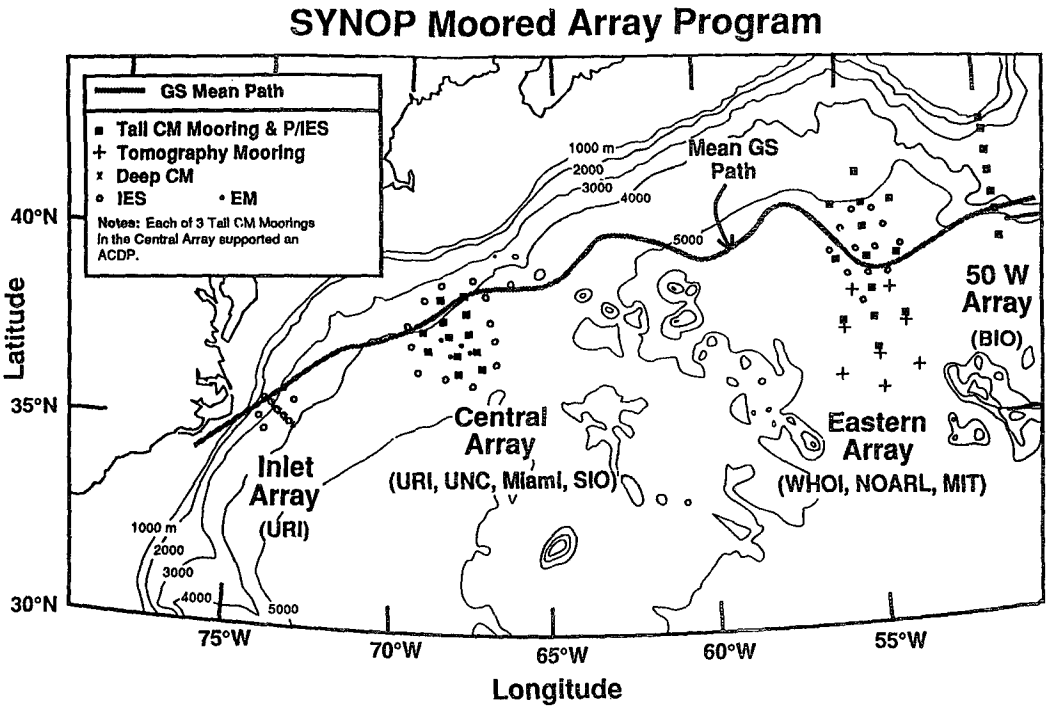

FIG. 1. Chart showing the region of the SYNOP field experiment and the location of moored arrays. CM: current meter, IES: Inverted Echo Sounder, P/IES: Inverted Echo Sounder with pressure sensor, EM: electro-magnetic field sensor, ADCP: Acoustic Doppler Current Profiler. [From *The Synoptician, 2(6),* December 1991.]

tions to examine the transport of the Gulf Stream and its recirculations between Cape Hatteras and the Grand Banks.

In what follows, we present three views of the Gulf Stream structure at 55°W. First, we have analyzed the data in a fixed, geographic coordinate system in order to compare the mean structure during SYNOP to a previous description by Richardson (1985) at this location. He used a combination of current meter, float, and surface drifter data from the 1970s and 1980s to produce sections of mean zonal velocity and eddy kinetic energy. The SYNOP data, which represent the first simultaneous velocity observations at both the thermocline and abyssal levels in this region, reveal some substantial differences related to interannual variability in the mean path of the Gulf Stream. The SYNOP data are also used to reexamine the estimates of total volume transport across 55°W by Niiler et al. (1985).

Second, we consider the structure of the Gulf Stream in a Lagrangian, or streamwise, coordinate system. Previous studies of the Gulf Stream structure in such a coordinate system at upstream locations have indicated that the current maintains a relatively fixed structure in spite of the lateral movements associated with meandering of the jet. Halkin and Rossby (1985, hereafter HR85) transformed 16 sections of absolute velocity and temperature made along a transect near 73°W into a coordinate system aligned with the instantaneous flow direction. They found that 1) the structure of the mean jet in stream coordinates was narrower and had higher downstream velocities than the geographical average section; 2) eddy kinetic energy in the streamwise coordinate system was one-third of that calculated in the fixed frame, indicating that most of the variability observed at 73°W is associated with meandering of a relatively fixed structure; and 3) a pattern of inflow from both sides of the stream, not apparent in the geographic average section, supports an increase in Gulf Stream transport in the downstream direction.

Johns et al. (1995; hereafter J95) have recently examined the velocity, temperature, and transport structure at 68°W based on the SYNOP Central Array data. Like HR85, they produced average sections of downstream and cross-stream velocity in stream coordinates. The mean downstream velocity sections from 68° and 73°W are shown in Fig. 2. As J95 point out, the similarity of the horizontal and vertical scales and peak downstream velocities at the two locations is remarkable. Both sections show the Gulf Stream to have about the same width, with higher shear on the cyclonic side of the current. The maximum in downstream velocity shifts offshore with depth, and there is a subsurface maximum in velocity on the offshore side at both locations. These results suggest that, at least as far east as 68°W, the average structure of the Gulf Stream viewed in stream coordinates remains relatively stable

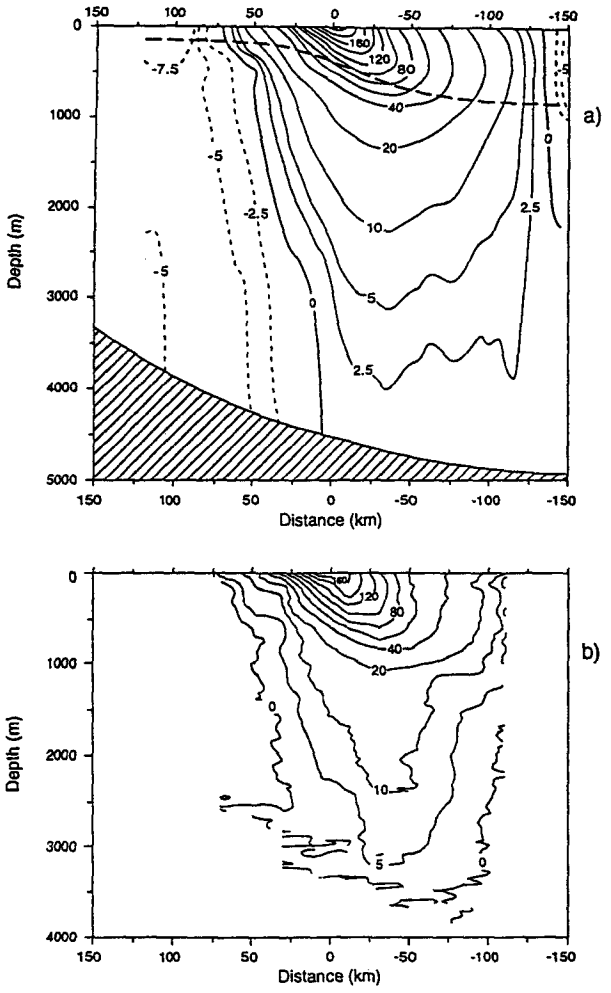

FIG. 2. Mean downstream velocity of the Gulf Stream (cm s^{-1}) at (a) 68°W (from J95), and (b) 73°W (from HR85). Negative velocity is indicated by dashed contours.

in spite of large amplitude meandering (the "wiggly hose" concept). The cross-stream velocity pattern at 68°W showed a significant inflow from the north, which J95 related to the influence of the Northern Recirculation Gyre (Hogg et al. 1986).

With the Eastern Array current meter data, we are in a position to extend the study of the "average synoptic" structure of the Gulf Stream farther downstream. By "average synoptic" structure, we mean the structure that is representative of the instantaneous Gulf Stream independent of its location. In an analysis of satellite altimeter data collected during the Geosat Exact Repeat Mission, Kelly (1991) found that the width of the average synoptic Gulf Stream at the surface is relatively constant between Cape Hatteras and the Grand Banks, while the sea surface height difference across the stream and the peak downstream velocity are greatest near 64°W and decrease east of that longitude. Here we examine the *subsurface* average synoptic structure and include an examination of the adjacent recirculation gyres in stream coordinates. We will also examine the pattern of cross-stream velocity and compare it to what has been observed upstream. Hogg (1992) has found that the mean transport of the Gulf Stream reaches a maximum, ~150 Sv (Sv ≡ 10^6 m^3 s^{-1}), at 60°W that is maintained to at least 55°W. This suggests that there may be no net inflow or outflow to the stream in this region.

The third view of the Gulf Stream at 55°W is the structure of eddy–mean flow interactions. Previous studies of transformations between the mean and eddy energy in the Gulf Stream have been restricted to locations upstream of the NESC, where the eddy energy is increasing rapidly in the downstream direction and where conversion of mean energy to eddy energy is expected (Rossby 1987; Dewar and Bane 1989; Hall 1986; Cronin and Watts 1996). In most of these studies, downgradient heat fluxes were observed and interpreted as the signature of baroclinic instability. Marshall and Shutts (1981) have pointed out, however, that in regions of strong advection of eddy potential energy (or equivalently, temperature variance), only the divergent part of the downgradient heat flux is related to the conversion of energy through baroclinic instability. The other, dynamically inert, part balances the downstream advection of eddy potential energy. Marshall and Shutts also point out that *upgradient* fluxes observed in regions of eddy decay do not necessarily indicate transfer of energy from the eddies to the mean at that location, but rather these fluxes balance the decrease in eddy energy following the mean flow.

Earlier observations at 55°W indicate that eddy energy is at a maximum, or perhaps decreasing in the downstream direction, depending on what depth is considered. Figure 3 shows the horizontal distribution of surface and abyssal eddy kinetic energy in the western North Atlantic. At the surface, the maximum in eddy kinetic energy appears to be upstream of 55°W, while at depth, the maximum, as well as it is resolved, includes the site at 55°W. In either case, a different signature of energy conversion is expected compared to upstream locations. If the Eastern Array is at the maximum in eddy energy, we anticipate no substantial cross-gradient fluxes or energy transformations. If this location is in a region of decreasing eddy energy, upgradient fluxes may be observed. The direction of the eddy heat and momentum fluxes can thus be used to determine where 55°W is in relation to the large-scale cycle of eddy growth and decay in the Gulf Stream.

In the next section, the basic experiment and the data processing methods are described. The three views of the Gulf Stream at 55°W based on the SYNOP data are presented and compared to other descriptions in sections 3–5. The results are summarized in section 6.

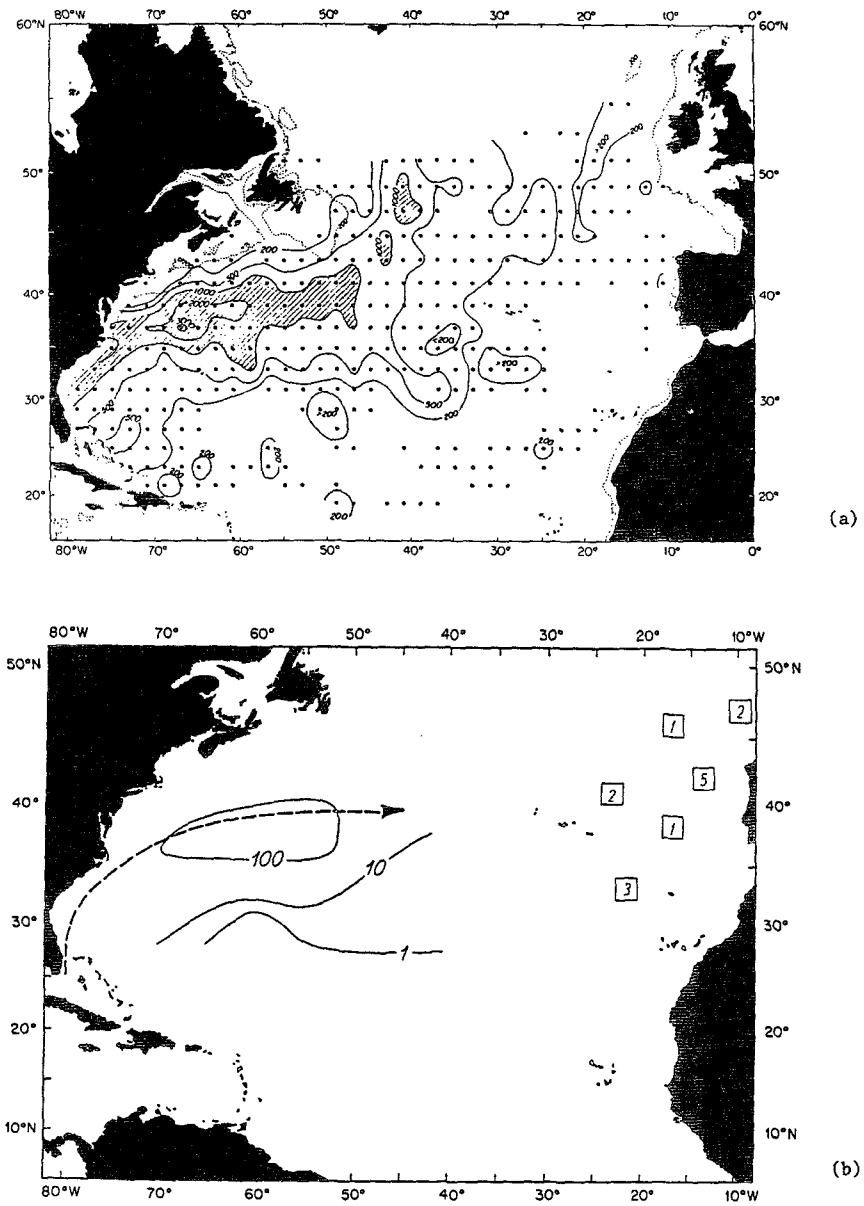

FIG. 3. Charts showing the distribution of eddy kinetic energy at (a) the surface, based on surface drifter data (Richardson 1983), and (b) abyssal level from historical current meter data (Schmitz 1984). (Units are $cm^2\ s^{-2}$.)

2. Data and methods

a. Experiment description

In October 1987, an array of 13 vector-averaging current meter (VACM) moorings were installed across the Gulf Stream near 55°W from the R/V *Knorr* as part of SYNOP. The array was recovered nearly two years later from the RRS *Charles Darwin* and approximately half redeployed for an additional two years, until finally recovered in July 1991 from the R/V *Oceanus*. In our analysis, we use data from the first setting only due to its broader geographic coverage. Data return from this setting was generally very good (see Table 1 for performance summary or Tarbell et al. 1993).

A plan view of the array is shown in Fig. 4. At 500 and 4000 m, there were current meters on all moorings. The moorings along the central north–south line, with the exception of the two extremes, had additional instruments at 1000 and 1500 m. The three moorings at each of the north and south extremes (numbers 1, 2, 3, 10, 11, 12) had extra instruments at 250 m to investigate the near surface structure of baroclinically unsta-

TABLE 1. Velocity and temperature data return rates.

Depth (m)	Velocity (%)	Temperature (%)
250	96	99
500	89	89
1000	72	92
1500	85	85
4000	94	94

ble disturbances believed to exist in the westward recirculations (Hogg 1985). Finally, the 500-m instruments on the central line had Seabird salinometers connected to the VACMs.

b. Data manipulation

After routine editing, the time series were filtered using a two-pole Butterworth filter with 40-hour half-power point and then subsampled once a day. The data were run through the filter both forward and backward to nullify any phase shifts.

The moorings were equipped with faring in the upper 400–500 m, and syntactic foam spheres at the top provided most of the buoyancy. Consequently, the downward movement of the topmost instrument was at most 250 m when the Gulf Stream passed over. Data from the 500-m level were corrected for this motion to a fixed depth of 550 m, and the 250-m data were also corrected using a scheme developed by Hogg (1991). The other depths were left unchanged.

Average spacing between the moorings was approximately 85 km, which is somewhat less than the expected eddy scale or the Gulf Stream width. Consequently, the array is marginally eddy resolving, and we have used the method of objective analysis (e.g., see Bretherton et al. 1976 or Daley 1991) to provide daily maps of the various property fields. With the additional assumptions that the spatial correlation function is homogeneous and isotropic and that the motions are quasigeostrophic, it is possible to incorporate all the measured variables, at a single level, into this mapping procedure (Bretherton et al. 1976; Hogg 1992). This has the advantage of reducing the formal mapping errors and allowing the temperature field to improve the velocity estimation between moorings (via the thermal wind relation) and vice versa.

c. Stream coordinate transformation

The methods used to determine the mean synoptic velocity structure of the Gulf Stream are similar to those described by J95. There are essentially three steps to the process. First, the location of the Gulf Stream axis must be defined for each day. Second, the downstream direction must be determined at each mooring site for every day, and third, the east and north velocity observations must be transformed into downstream and cross-stream components and along with temperature, binned according to cross-stream position (distance from the axis) and averaged.

In J95 and the present study, the Gulf Stream axis is defined to be coincident with the location of the 12°C isotherm at a specified depth, but the method used to determine the location of the axis was slightly different in the two studies. At 68°W, the current meter array was augmented by an extensive set of Inverted Echo Sounders (IESs) that was used to map the depth of the 12°C surface throughout the Central Array on a daily basis. J95 used these maps to locate the Gulf Stream axis, defined as the 400-m contour of these maps. An array of IESs was also installed at 55°W by the Naval Oceanographic and Atmospheric Research Laboratory as part of their Regional Energetics Experiment (REX) (Hallock 1992). Unfortunately, this array was only in place for the first nine months of the two-year current meter deployment and therefore cannot be used to map the Gulf Stream path during the full two years. However, as described in the previous subsection, daily objective maps of the temperature field at 550 m were produced using the velocity and temperature data from the current meters, and these maps were used to locate

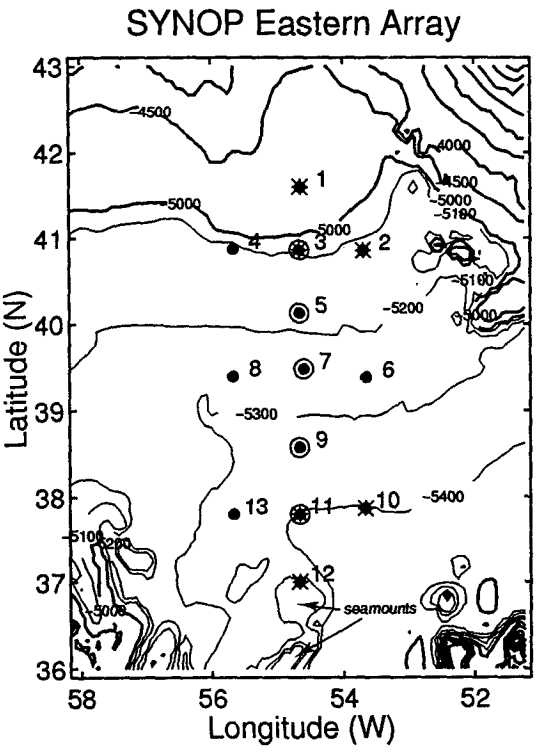

FIG. 4. Detailed chart of the current meter mooring locations in the Eastern Array (first setting). Bold contours are every 500 m, and thin contours are added every 100 m between 5000 and 5400 m. Solid dots: current meters (CMs) at 500 and 4000 m, O: current meters at 1000 and 1500 m, *: current meters at 250 m.

the Gulf Stream axis, defined in this case as the 12°C contour at 550 m. This axis lies slightly seaward of the axis defined by J95 owing to the slope of the thermocline across the Gulf Stream, but in both cases, the axis is located near the middle of the strong temperature gradient associated with the Gulf Stream's baroclinic front.

Most of the remaining steps in the coordinate transformation process are quite similar to those used by J95, and the reader is referred to that reference for more details. It is worth discussing briefly, however, the method for defining the downstream direction at each mooring site. The exact choice of the downstream direction has relatively little effect on the structure of the mean *downstream* velocity in stream coordinates, but the impact on the *cross-stream* component, and the interpretation of that component in terms of transport increase or decrease in the downstream direction, is more significant. HR85 defined the downstream direction along each of the Pegasus sections at 73°W to be parallel to the vector average of the three largest transport/unit width vectors in the center of the Gulf Stream. When the observed velocities were rotated into downstream and cross-stream components and averaged together, a mean flow toward the axis of the stream from both sides was found, which HR85 interpreted as indicative of a convergence of transport streamlines and increasing transport in the downstream direction.

At about the same time, Hall (1986) developed a method for examining the average synoptic structure of the Gulf Stream with a single current meter mooring. In her study, the downstream direction was defined daily to be parallel to the vertical shear between current meters spanning the thermocline. For geostrophic flow, this is the direction of the "thermal wind" and is parallel to contours of dynamic height integrated between the observation levels. Hall used this method to examine the structure of downstream velocity. The horizontal structure of the cross-stream component was not explored.

In their analysis of the SYNOP Central Array data, J95 also used this method (which we will refer to as the shear method) to define the downstream direction locally (at each mooring site) on each day for moorings that were clearly in the strongly sheared flow of the Gulf Stream. To extend the analysis outside the jet itself, however, J95 used a different method, where the downstream direction at each mooring site was defined to be perpendicular to a line drawn between the site and the closest point on the axis (12°C at 400 m). This is referred to as the mapping method because it depends on the use of the objective maps of temperature. J95 attempted to use the mapping method throughout, but they found it produced noisier results than the shear method within the jet itself. The result of their combined shear and mapping methods indicated a strong inflow to the Gulf Stream from the north, which they interpreted as a concentrated flow from the northern recirculation gyre.

We have explored both mapping and shear methods for defining the downstream direction at the mooring sites in the Eastern Array. Although we too find that the shear method gives a smoother pattern of cross-stream velocity, it appears that the two methods are not measuring the same thing, and in particular, the shear method may not be suitable for estimating inflows or outflows associated with increasing or decreasing Gulf Stream transport. This will be discussed in more detail in the results section.

To remove data in warm and cold core rings, J95 used a hand-editing procedure based on the IES maps to flag observations associated with rings, while we have used a more automated approach. The best indicator of the presence of a ring in the data is temperature at 550 m. This is illustrated in the top panel of Fig. 5, which shows the scatterplot of temperature at 550 m from all moorings as a function of cross-stream distance. In the lower two panels, the corresponding standard deviation and the number of observations in each 20-km bin are shown by the solid white lines. The strong cross-stream temperature gradient associated with the Gulf Stream front is clearly evident between ±50 km from the center. The standard deviation indicates a minimum at the center of the jet, which is ex-

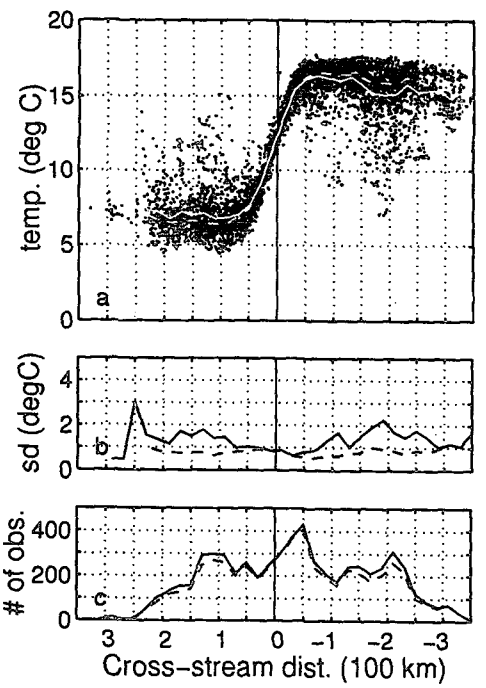

FIG. 5. (a) Scatterplot of temperature at 550 m in the stream coordinate system before ring observations were removed. White lines indicate 20-km binned means before (solid) and after (dashed) ring data were removed; (b) standard deviation of temperature before (solid) and after (dashed) rings were removed; (c) as in (b) but showing the number of observations per 20-km bin.

pected since the axis ($y = 0$ km) is defined in terms of temperature to be where the 12°C isotherm is at 550 m. If it were not for the fact that the objective analysis smooths the temperature field slightly, the standard deviation at the origin would be zero by definition.

The standard deviation is almost twice as large to the north and south of the stream as it is near the center, and the scatterplot clearly indicates the influence of rings in producing this elevated variability. On the south side of the axis, for example, the points cluster around 16°C, but there are many points at significantly colder temperature. These are temperatures measured in cold core rings. Likewise on the north side, large anomalies are all positive (warm), indicative of warm core rings there. To eliminate the influence of rings on the mean structure, velocity and temperature data associated with these outliers were removed from the analysis. On the north side of the stream, data from a mooring was flagged on days when the temperature at 550 m was more than 1.5°C warmer than the mean, and similarly for the moorings south of the stream, data were not used on days when the temperature at 550 m was more than 1.5°C colder than the mean. The dashed lines in Figs. 5b,c show that the standard deviation has a more uniform distribution after the rings were removed and that the number of points eliminated by this process is not significant. This method is effective at removing data from near the center of rings, where the temperature anomaly is largest. Some observations from near the edges of rings, where the temperature anomaly is small but the velocity anomaly is large, were probably missed by this editing procedure.

3. Geographic coordinate analysis

a. Horizontal structure at 550 and 4000 m

Since the 500-m and 4000-m levels were the most heavily instrumented, we first present the mean velocity vectors and mean temperature (average of daily objective maps) at these depths (Fig. 6). The boxes around each velocity vector in Figs. 6a,c indicate the 95% confidence level using a decorrelation timescale of 7.5 days (J95). Note that both temperature and velocity observations and information on their errors have been objectively analyzed in a dynamically consistent way to produce the contoured maps of mean temperature, resulting in some small differences between the measured mean temperatures at each mooring site and the mean of the objective maps (e.g., see Fig. 6d, southern moorings).

The mean eastward flow of the Gulf Stream is the most prominent feature at 550 m, Fig. 6a, with maximum speed of about 30 cm s^{-1} in the center of the array. The flow field is not purely zonal but has some cyclonic curvature that is statistically significant. North of the mean stream, there is little evidence of a westward flow associated with the northern recirculation gyre in this coordinate system; only one mooring (number 3) shows a westward mean velocity vector and it is not significantly different from zero. Immediately south of the mean Gulf Stream ($y = -200$ km), there is no significant mean flow to the west that would be indicative of a southern recirculation there, although the ridge of higher temperatures at $y = -200$ km is consistent with the presence of a westward geostrophic flow south of that latitude (assuming a deep level of no motion). The marginally significant southward component of the mean flow at the southern most mooring is probably a small-scale feature associated with a minor seamount near the mooring site (see location of mooring number 12 in Fig. 4 and in Fig. 7 below).

At 4000 m, Figs. 6c,d, the eastward flowing Gulf Stream no longer dominates the circulation as it did at the thermocline level. Maximum eastward speed near the center of the array is about 5–6 cm s^{-1}, but mean westward speeds up to 8 cm s^{-1} are found north of the stream. The strong and significant northward component at mooring 6 is suggestive of a continuous cyclonic circulation feeding into the westward flow. To the south of the eastward jet, the dominant feature is the southeast flow at mooring 12, which appears to be steered and enhanced locally by the presence of the seamount mentioned above. As at 550 m, there is no evidence of westward recirculation in the velocity field south of the Gulf Stream, but there is a ridge of higher temperatures at moorings 9, 10, 11, and 13 compared to mooring 12.

b. Vertical structure

The mean zonal velocity distributions at 550-m and 4000-m depths have been combined with the results from 250, 1000, and 1500 m to produce a meridional section of eastward velocity, Fig. 7a. Also included in this section are the mean surface velocity observations at 54.5°W reported by Kelly (1991), which were inferred from sea surface height measured during the 2.5-year Exact Repeat Mission of Geosat. These observations of the mean cross-track speed in the direction 072°T, taken between November 1986 and April 1989, overlap substantially with the deployment of the Eastern Array current meters.

To examine the section of mean zonal velocity in the context of previous observations, the section of mean eastward velocity from Richardson (1985) is shown to the same scale in Fig. 7b. It is important to point out that the Richardson section was constructed using a variety of data types collected over a seven year time span, including surface drifters (1977–1980), SOFAR floats at 700 and 2000 m (1980–1982), and current meters from the POLYMODE Array II experiment (1975–1977). Note that Richardson estimated the wind drift at the surface and removed it from this mean section.

The SYNOP data reveal a mean zonal jet that is generally narrower, stronger, and more vertically aligned

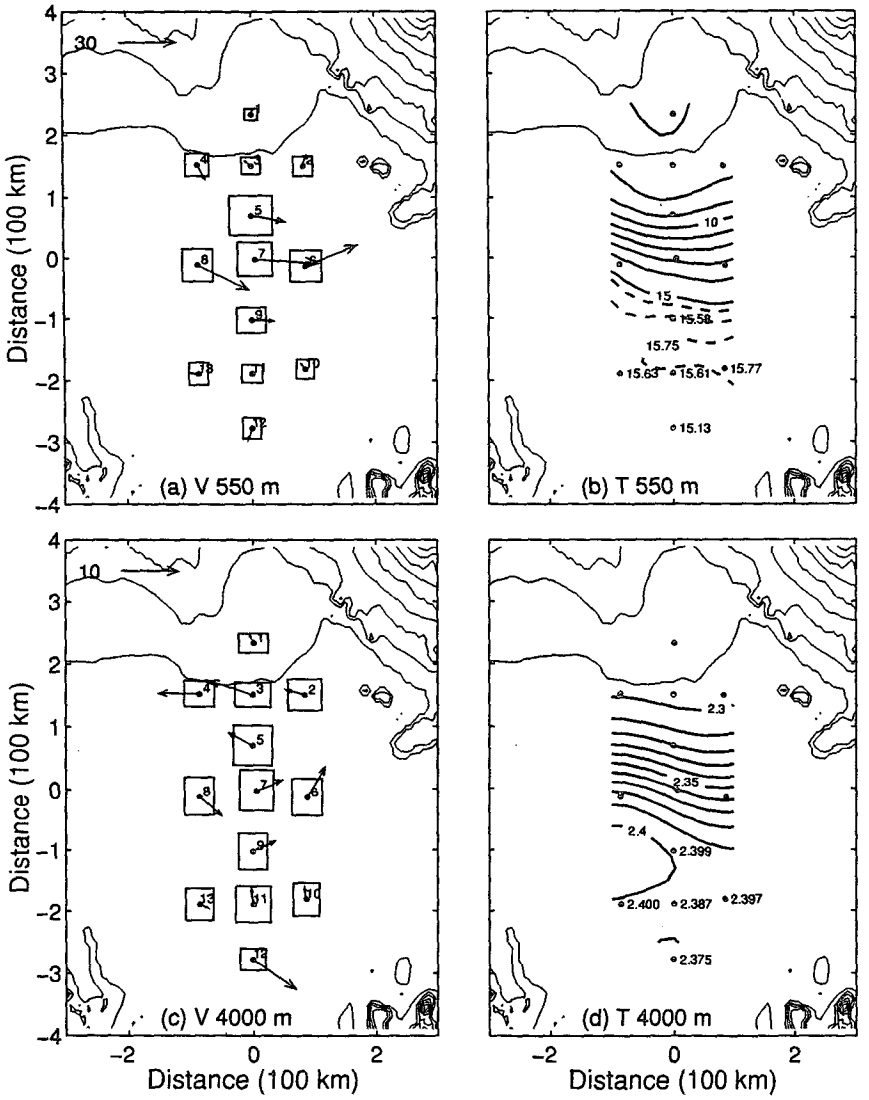

FIG. 6. (a) Mean velocity vectors and (b) mean temperature contours (from objective analysis) at 550 m. Scale for the velocity vectors is in the upper left corner in cm s^{-1}. Temperature contour interval is 1°C, except the dashed contours which are at 0.25°C intervals, and individual observed mean values are given for southern moorings. Mooring numbers are indicated. (c) As in (a) but for 4000 m; (d) As in (b) but for 4000 m. Contour interval is 0.01°C.

than that in the Richardson section. The width of the eastward flowing jet at the surface is about 400 km during SYNOP, compared to about 800 km in the earlier section. At depth, there is no significant mean westward flow south of the eastward jet during the SYNOP time frame: the mean flow is eastward all the way to the southern limit of the array (37°N). The Richardson section, which extends farther to the south, shows eastward flow to about the same latitude, flanked by a westward return flow south of about 37°N. The peak velocity at the surface was between 35 and 40 cm s^{-1} during SYNOP (from GEOSAT), about 10 cm s^{-1} greater than in the Richardson section (from surface drifters). Furthermore, the 10 cm s^{-1} contour reaches to 1000 m during SYNOP and only 700 m in the Richardson section.

The SYNOP section also indicates a jet that is much more vertically aligned than in the Richardson section. At both surface and 4000 m, the velocity maximum during SYNOP is located between 39° and 40°N. In the Richardson section, the surface maximum is found at about the same latitude, but the deep maximum is displaced more than 1° to the south relative to the surface maximum. Since the current meter data used by Richardson to estimate mean velocity at 4000 m was collected during the two years prior to the time of the surface drifter mea-

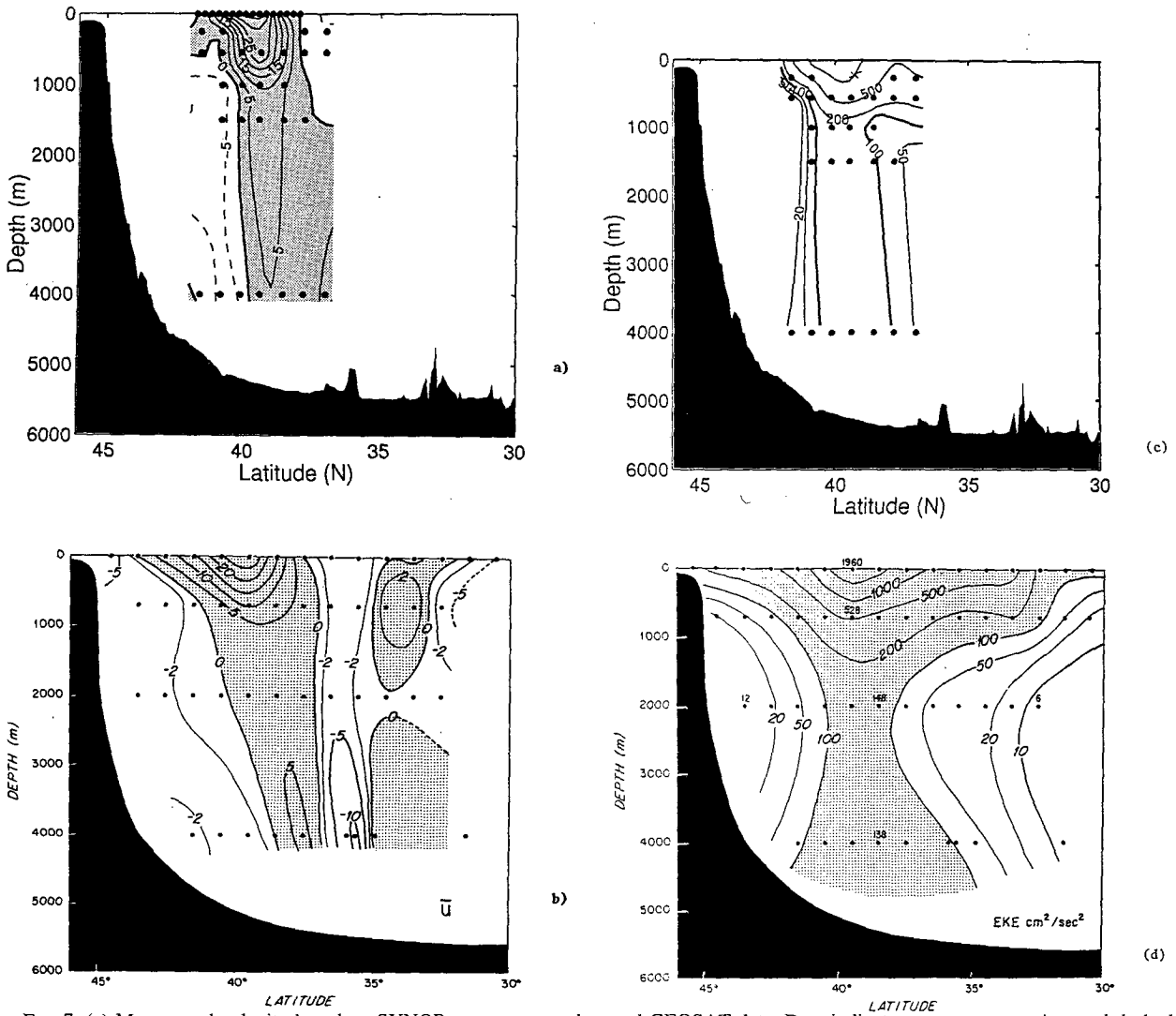

FIG. 7. (a) Mean zonal velocity based on SYNOP current meter data and GEOSAT data. Dots indicate measurement points and dashed contours indicate westward velocity; (b) mean zonal velocity reproduced from Richardson (1985); (c) eddy kinetic energy from SYNOP current meter data; (d) eddy kinetic energy from Richardson (1985).

surements, it seems plausible that this large shift of the velocity maximum with depth is the result of low-frequency temporal variability in the mean path of the Gulf Stream. In fact, Richardson (1985) shows the cross-stream profiles of eastward velocity for each of the three 9-month settings of the POLYMODE Array II moorings, and the peak velocity at 4000 m shifts from 39°N in the first setting to 38°N in the second setting and 37°N during the third setting. In light of the fact that the SYNOP observations, which were collected simultaneously at the thermocline and abyssal levels, show a vertically aligned jet, we conclude that the shift in the velocity maximum in the Richardson section is most likely an artifact of the non-contemporaneous nature of the data used at the different levels.

The structure of eddy kinetic energy (EKE) is similar in the two realizations (Figs. 7c,d). Maximum values of 1000 $cm^2\ s^{-2}$ are indicated near the surface. At 4000 m, EKE exceeds 100 $cm^2\ s^{-2}$ in both sections, although the extent of these maximum values is greater in the Richardson section. Again, this is most likely due to the more southerly positions occupied by the Gulf Stream during the POLYMODE Experiment.

c. *Total transport across 55°W*

Niiler et al. (1985) used the POLYMODE current meter data, along with contemporaneous hydrographic data, to estimate the total volume flux across 55°W between 33° and 42°N. Relative to the bottom two different

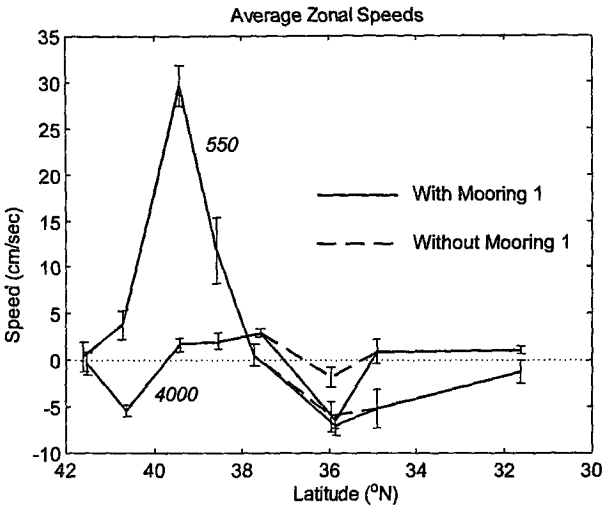

FIG. 8. Mean zonal velocity at 550 and 4000 m from a combination of SYNOP and POLYMODE data with (solid) and without (dashed) one of the POLYMODE moorings included (see text).

hydrographic sections gave nearly identical estimates of about 31 Sv. To obtain the absolute transport, the POLYMODE current meter data at 4000 m were used. A trapezoidal integration of the mean zonal velocity component at this depth gave them -1.3 ± 0.6 Sv/100 m. When applied to the whole water column, this gives a depth-integrated total transport of -47 ± 36 Sv (i.e., to the west), in apparent disagreement with a value of 10 Sv to the east that they obtain from the Sverdrup relation using Leetmaa and Bunker (1978) wind stress data to the east of the 55°W section. They speculate that the Sverdrup relation may be inappropriate or that the mean flow was not adequately resolved by the moorings.

Using the combined SYNOP–POLYMODE dataset, we have more information with which to reference the hydrographic sections. Figure 8 shows the zonal current component at 550-m and 4000-m depths averaged over bins of 1° in latitude. The Gulf Stream and its recirculations are obvious. However, in using all the available data, a strong westward flow exists at both depths near 36°N. Owens and Hogg (1980) suggested that a small seamount located near 36°N, 55°W has a strong influence on the local currents through the production of an anticyclonic Taylor column. Therefore, we have calculated the mean zonal speed distribution both with (solid line, Fig. 8) and without (dashed line) data from the single mooring closest to the seamount. The distribution without these data is smoother and more visually compelling. The two estimates of transport per unit depth that result from integrating the mean zonal component at 4000 m are -0.54 ± 0.67 Sv/100 m (with POLYMODE mooring 1) and 0.35 ± 0.79 Sv/100 m (without POLYMODE mooring 1). Both of these are more positive than the Niiler et al. estimate, although only the latter is significantly so (based on the standard error estimates).

In Fig. 9, we add these estimates to the figure from Niiler et al., which shows the vertical distribution of the latitudinally integrated baroclinic transport using the Niiler et al. estimate of the 4000-m velocity (solid line). The combination of the 550-m and 4000-m direct current estimates from SYNOP and POLYMODE would suggest a shift to the right (dashed line). Consistent with this, we calculate a mean transport across 55°W of 3 ± 35 Sv (with mooring 1) or 49 ± 41 Sv (without mooring 1), neither of which is now inconsistent with the 10 Sv estimated from the Sverdrup relation. We conclude that the Sverdrup relation cannot be questioned based on this combined dataset.

4. Stream coordinate analysis

a. Downstream velocity

Figure 10 shows all observations of the downstream velocity component at 550 (Fig. 10b) and 4000 m (Fig. 10d) after transforming the east and north velocity components into stream coordinates and applying the quality control criteria discussed in section 2 (e.g., rings have been removed). The mean profiles after averaging in 20-km bins are shown by the solid lines, and

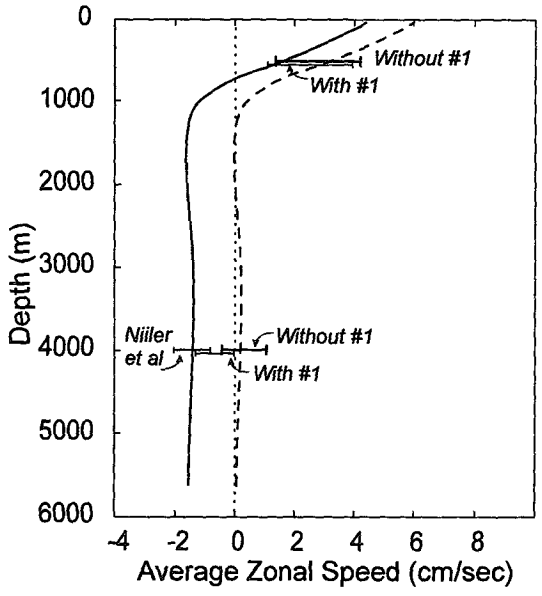

FIG. 9. Transport per unit width from Niiler et al. (1985) (solid line), with correction based on SYNOP/POLYMODE current meter data (dashed line). The correction is determined by adjusting the velocity profile, which was based on the dynamic method, to the average velocity determined by direct velocity measurements at 550- and 4000-m depths (horizontal error bars), using the combined POLYMODE and SYNOP East datasets, with (thin error bars) and without (thick error bars) POLYMODE mooring 1 (see text). At 4000 m the leftmost error bar is the one based on the POLYMODE measurements alone, as given by Niiler et al. (1985).

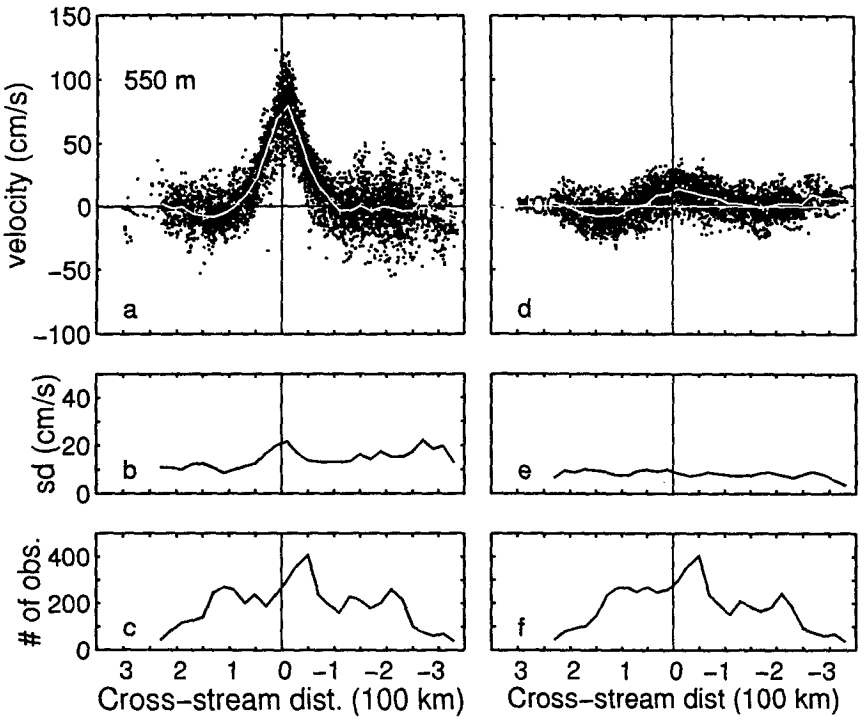

FIG. 10. (a) Scatterplot of downstream velocity at 550 m after data from rings were removed, with (b) standard deviation about the mean in each 20-km bin and (c) number of observations per bin. (d–f) Same as in (a–c) but for 4000 m.

the cross-stream distributions of standard deviation and the number of observations for each bin are shown in the lower panels. The number of observations per bin is typically between 200 and 300. At 550 m, the standard deviation is about 10 cm s^{-1} north of the stream axis, increasing to a maximum of 20 cm s^{-1} in the center of the jet and then returning to values between 10–15 cm s^{-1} to the south. At 4000 m, the rms variability is more uniform across the jet, with typical values of about 10 cm s^{-1}.

The mean velocity profiles in stream coordinates from all four depths are shown on the left in Fig. 11 (solid lines), along with the profiles of mean eastward velocity in the geographic frame (dashed lines). The maximum downstream velocity in stream coordinates was found to be about 75 cm s^{-1} at 550 m, decreasing to about 15 cm s^{-1} at 4000 m. At all levels, the maximum in stream coordinates is about two times larger than that in the fixed frame. The average synoptic jet at 550 m appears to be symmetric about the axis, with a total width of about 200 km. The northern edge of the jet shifts to the right with increasing depth, producing a more asymmetric jet structure at 4000 m compared to 550 m. The total width is approximately the same at all depths.

The stream coordinate analysis reveals a counterflow north of the Gulf Stream at all four depths that is quite barotropic and has peak velocities of about 8 cm s^{-1}. This feature was completely absent at 550 m in the geographic frame. At 550 and 4000 m, the full width of the counterflow, about 130 km, is resolved. South of the Gulf Stream, the mean counterflow is much weaker, with slight surface intensification.

The panels on the right in this figure show eddy kinetic energy in the two coordinate systems. At 550 m, EKE in the center of the average synoptic jet (solid line) is five times less than EKE measured in the geographic frame (dashed line). At the deeper levels, the decrease in EKE achieved by the transformation to stream coordinates is less. Because the external eddy field is more depth independent than is the Gulf Stream, the transformation to stream coordinates has more impact at 550 m than 4000 m.

The velocity profiles from all four depths are combined in one plot, Fig. 12a, to emphasize the vertical structure of downstream velocity. Note that there is no *resolvable* shift of the velocity maximum with depth: the maximum is observed in the same cross-stream bin at all depths. At 73° and 68°W, most of the offshore shift in the velocity maximum (~30 km) was observed between the surface and 500 m (see Fig. 2). Below that depth, the maximum shifts only about 10 km further offshore. With the 20-km bin size at 55°W, we would be unable to detect a shift of the velocity maximum of this size.

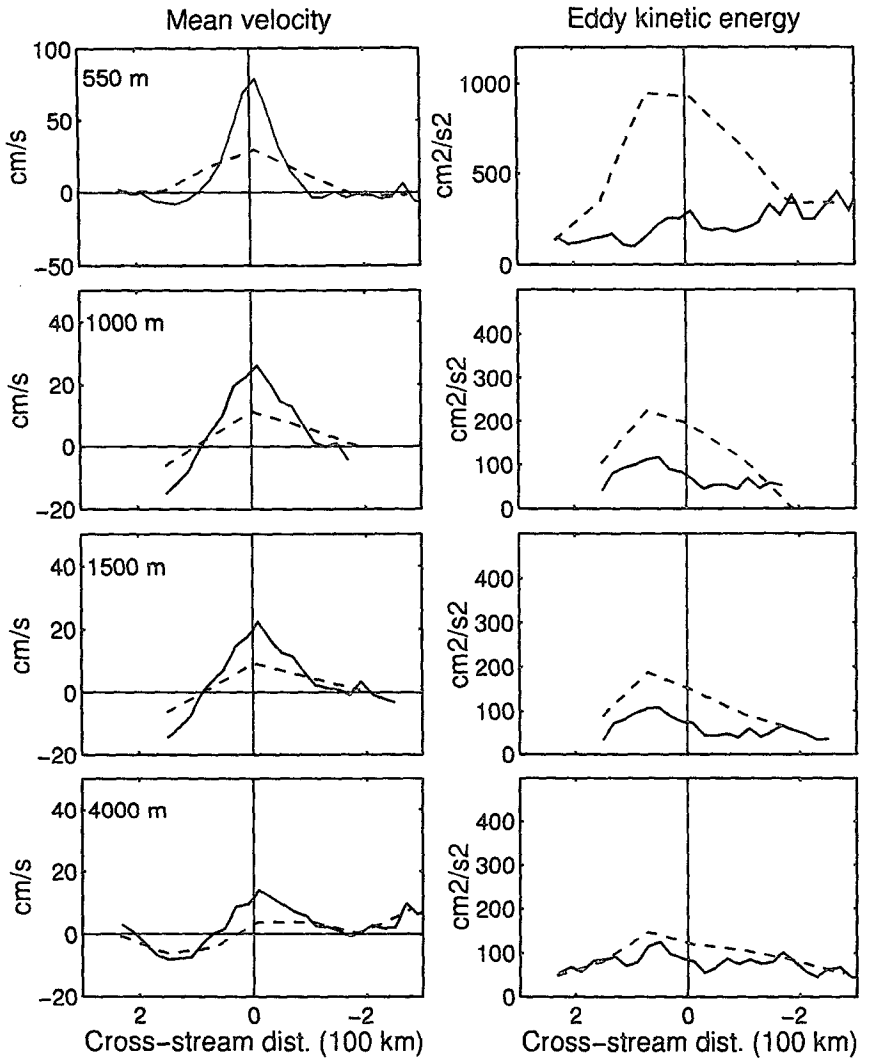

FIG. 11. Mean velocity (left-hand panels) and eddy kinetic energy (right-hand panels) at four measurement levels in stream (solid) and geographic (dashed) coordinates.

The transport of the average synoptic Gulf Stream at 55°W has already been estimated by Hogg (1992) to be about 150 Sv, based on the same data being analyzed here. He combined this estimate with others from various locations in the Gulf Stream system to develop a picture of the total transport streamfunction for the northwestern North Atlantic. To conserve mass, he inferred that the transport of the northern recirculation gyre (NRG) was about 60 Sv, which included 15 Sv associated with the deep western boundary current (DWBC) that flows westward along the continental slope at the northern edge of the gyre (see his Fig. 13). The present stream coordinate analysis, using the mapping method, allows us to estimate the transport of this recirculation directly. If we average the counterflow north of the Gulf Stream at 550 and 4000 m (the two levels that fully resolved the return flow), integrate in the cross-stream direction to include all the counterflow north of the stream, and multiply by 5000 m (which assumes the flow is barotropic), we obtain a transport of about 32 Sv. This estimate probably does not include the flow of the DWBC, since all the observations were made seaward of the main core of that current, which is typically centered over the 3500-m isobath (Pickart 1992).

This estimate of the return flow transport north of the stream is surprisingly low compared to what is expected from Hogg's (1992) inferred estimate of 45 Sv (60–15 Sv of DWBC). It is even lower than Richardson's (1985) estimate of 41 Sv, which, as he points out, is probably biased low by the Eulerian averaging technique used to make the estimate. The apparent discrepancy can be explained if one considers what exactly our estimate of 32 Sv represents. It is the average

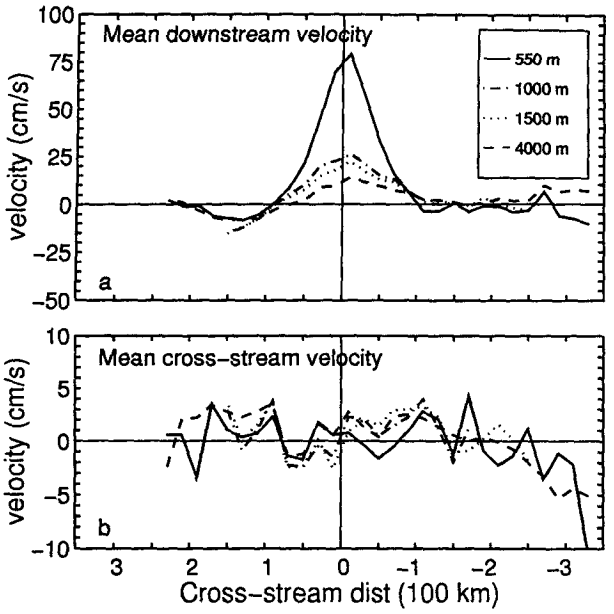

FIG. 12. (a) Mean downstream velocity at four depths in stream coordinates; (b) mean cross-stream velocity.

transport associated with the flow that is opposite *but parallel* to the Gulf Stream direction. If the direction of the flow of the NRG is in general to the west, rather than parallel to the instantaneous direction of the Gulf Stream, the stream coordinate technique will underestimate the transport associated with the NRG. If we integrate the mean *zonal* velocity, rather than the alongstream velocity, including all the *westward* flow north of the *downstream* flow of the Gulf Stream, we obtain a transport of 42 Sv, which is more in line with Hogg's and Richardson's estimates. The conclusion is that the counterflow north of the stream is not, on average, parallel to the instantaneous path of the Gulf Stream, but rather flows generally westward, parallel to the topography.

b. *Cross-stream velocity*

The cross-stream velocity computed via the mapping method, Fig. 12b, has a lower signal to noise ratio than the downstream velocity. In Fig. 13 (left panels), the cross-stream structure of mean cross-stream velocity is shown for each observation level with 95% confidence intervals about the mean, and it is apparent most of the estimates are not significantly different from zero at the 95% confidence level. However, there is some evidence of a consistent pattern at the 1000-m level and below, with negative cross-stream velocity on the north flank of the jet, between about +75 and 0 km, and positive velocity on the southern side between 0 and −150 km. This is indicative of cross-stream flow *toward* the Gulf Stream axis from both sides, but with the large error bars, one must question the significance of this pattern.

Johns et al. (1995) also found that cross-stream velocity at 68°W was noisy when the mapping method was employed, a result, they claim, of the smoothing inherent in the objective analysis of the temperature maps. They found that when the shear method was used to determine downstream direction at the mooring sites, the noise in cross-stream velocity was substantially reduced. With the hope of a similar improvement in the signal to noise ratio, the shear method was applied to the Eastern Array data, and the results are illustrated in Fig. 13 (right panels). This method can only be used in the main downstream jet, where there is measurable vertical shear, so the cross-stream extent of the estimates is reduced using this method. Also, since the downstream direction is defined to be parallel to the shear between 550 and 1500 m, the mean cross-stream velocity structure at these two depths is identical.

A relatively consistent pattern of inflow on both sides of the stream appears at all depths using the shear method, and it is somewhat smoother across the jet than what was found using the mapping method, but the error bars still indicate that most of the estimates of the mean are not significantly different from zero. But the relatively smooth pattern of cross-stream velocity has compelled us to examine it in more detail. When either the shear method or the mapping method is used, cross-stream velocity is related to the turning of the current vectors with respect to some definition of the downstream direction. In the shear method, the downstream direction is defined as parallel to the direction of vertical shear between the 550-m and 1500-m levels. If these vectors are parallel, cross-stream velocity is identically zero at both of these depths.

Turning of the current with depth is a common feature of Gulf Stream velocity observations. Most recently, Lindstrom and Watts (1994) have documented it in the Central Array data and shown that the direction of turning is related to the dynamics of meander phase propagation, with currents turning counterclockwise with increasing depth between meander troughs and crests, and vice versa between crests and troughs. A similar pattern is apparent in the Eastern Array data. In Fig. 14, the direction of the velocity vector at 1500 m is plotted as a function of the flow direction at 550 m for all the observations used in the shear method. If the flow at these two depths was always parallel, all the points would fall on the $y = x$ line shown in the figure. But, in fact, the points fall off the line in a somewhat systematic pattern. When the current direction at 550 m is between east and north (between trough and crest), the current direction at 1500 m is in general more positive than that at 550 m, or the current turns counterclockwise with depth (see Fig. 15). When the flow at 550 m is between east and south (between crest and trough), the direction of the flow at 1500 m has a tendency to be more toward the south; that is, the current turns clockwise with depth, although there are more exceptions in this case than for the northeast flow.

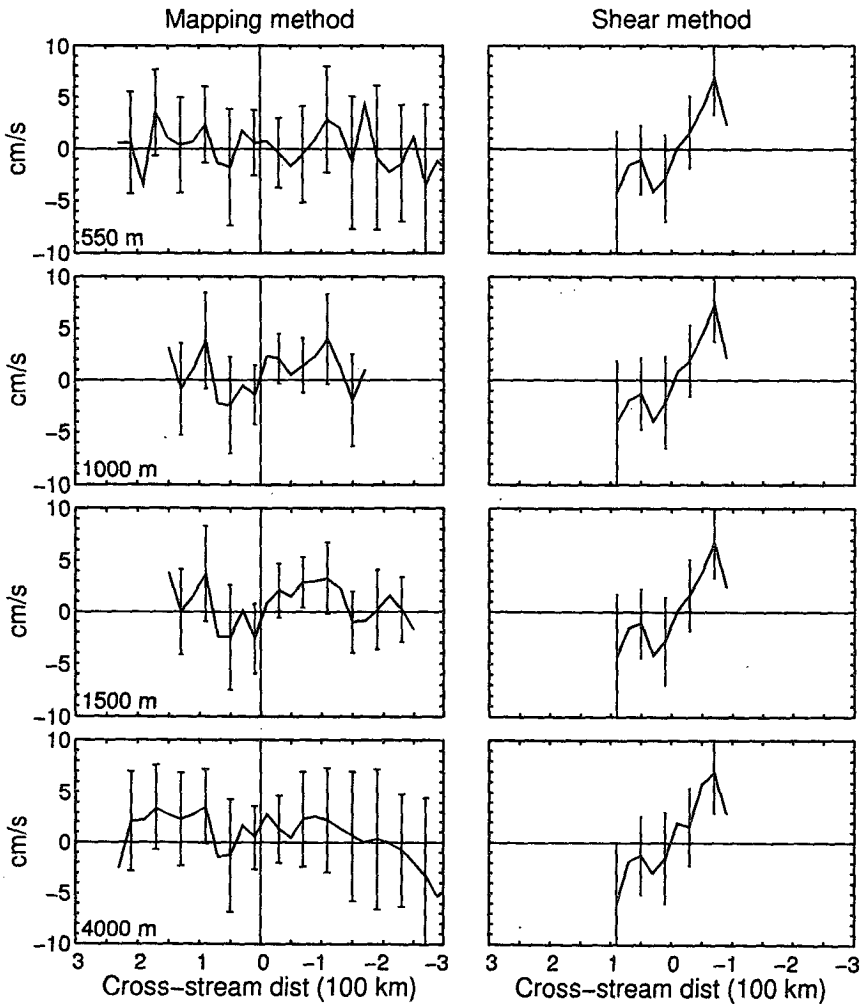

FIG. 13. Mean cross-stream velocity at four depths using the mapping method (left panels) and the shear method (right panels). Error bars indicate 95% confidence intervals.

Using our definitions, the counterclockwise turning with depth that is predominantly observed when the current is flowing toward the northeast implies a positive cross-stream velocity (to the left facing downstream), while clockwise turning, observed mostly when the flow was southeast, implies negative cross-stream velocity. This relationship between cross-stream velocity and meander phase is illustrated in Fig. 15, where the observations of cross-stream velocity have been divided by direction of flow at 550 m and side of the stream. The mean values, 95% confidence intervals, and number of observations are shown for each quadrant. The significant positive values on both sides of the stream in the northeast flow reflect the consistent pattern of counterclockwise turning with depth shown in the previous figure for this flow direction. Negative cross-stream velocity (inflow) of about the same magnitude (within the uncertainty) is indicated between crest and tough on the north side of the stream axis, while the direction of flow south of the axis is indistinguishable from zero based on the large variability in this quadrant.

These results indicate, especially in the flow from trough to crest, that cross-stream velocities calculated using the shear method are correlated with meander phase, with positive velocity between troughs and crests, and negative velocity between crests and troughs. This leads us to question the appropriateness of using this method to estimate the inflow or outflow associated with transport increase or decrease. To detect such an inflow or outflow, one must measure the component of flow toward (or away from) the axis of the stream, which should be defined in terms of the transport vector, such as was done by HR85. The shear method calculates the component of flow perpendicular to a *local* definition of "downstream," namely, the direction of vertical shear *at that mooring site.* The mapping method, which uses the objective maps to define

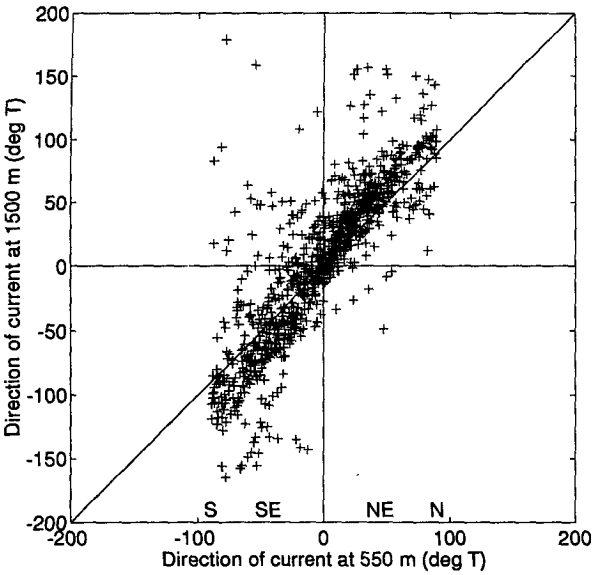

FIG. 14. Scatterplot showing flow direction at 550 m versus direction at 1500 m for data used in the shear method. The diagonal line represents $x = y$.

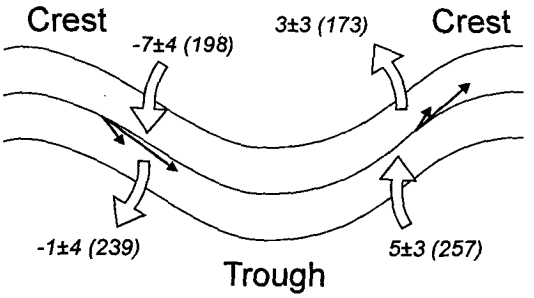

FIG. 15. Schematic diagram of a Gulf Stream meander showing turning of the current with depth (solid vectors) between meander extrema and pattern of cross-stream velocity observed using the shear method (outlined vectors). Mean cross-stream velocity in each quadrant is shown (in cm s^{-1}) with 95% confidence intervals. Number of observations used in each estimate of the mean is given in parentheses.

the axis and estimates cross-stream velocities *relative* to that axis, represents a better method for exploring inflow and outflow as it relates to transport changes. Therefore, considering the results only from the mapping method, we conclude that there is no evidence of inflow to or outflow from the Gulf Stream at 55°W, consistent with Hogg's (1992) finding that Gulf Stream transport is at a maximum at 55°W.

c. *Downstream development of the average synoptic structure of the Gulf Stream*

In Fig. 16, a vertical section of the average downstream velocity at 55°W is shown to examine the changes in the average synoptic Gulf Stream in the downstream direction between 73° and 55°W (compare this figure with Fig. 2). At the thermocline level, the width of the downstream flow is about the same at all three site (175–200 km), and the peak velocities are comparable. Below the thermocline, the width of the anticyclonic side of the jet appears to increase at 68° and 55°W, where the zero velocity point is beyond the measurement area. The most striking difference between the sections, however, is the significantly larger downstream velocities found at depth at 55°W compared to the upstream locations. This is most apparent in the location of the 10 cm s^{-1} contour, which extends to 4000 m at 55°W and only to 2000 m at 68°W. This feature was also noted by Hogg (1992) in terms of barotropic transport increases between Cape Hatteras and 55°W.

In Fig. 17, we have plotted downstream velocity at 550, 1000, and 1500 m at 73° (dashed lines) and 55°W (solid lines) with the 95% confidence intervals for the Eastern Array estimates. The origin of the cross-stream coordinate at 73°W had to be shifted 7 km to the left to line up with the axis as it has been defined at 55°W. At 550 m, the peak velocities and the jet width are the same within the 95% confidence interval of the mean at 55°W, although the jet at 55°W is more symmetric than at 73°W. These results suggest that the same peak velocity is maintained in the thermocline as far east as 55°W. This is a somewhat different result than what was reported by Shaw and Rossby (1984). They noted an approximate 25% decrease in the peak velocity in the Gulf Stream at the thermocline level east of about 58°W, but this was based on a small number of SOFAR

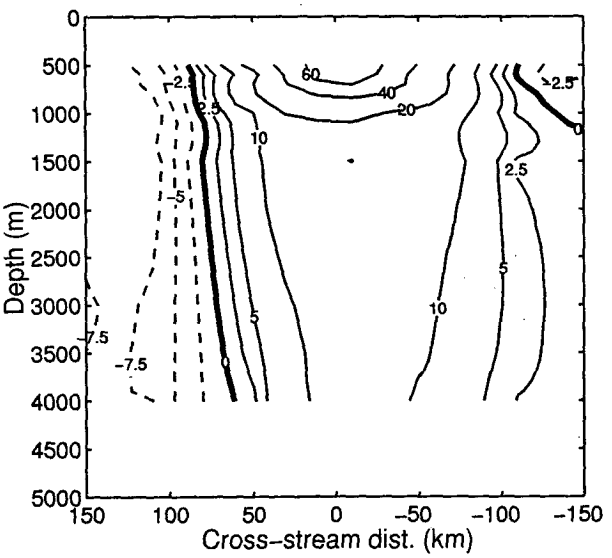

FIG. 16. Section of mean downstream velocity in stream coordinates at 55°W from SYNOP Eastern Array data. Contour interval is same as for Fig. 2a. (Units are cm s^{-1}.)

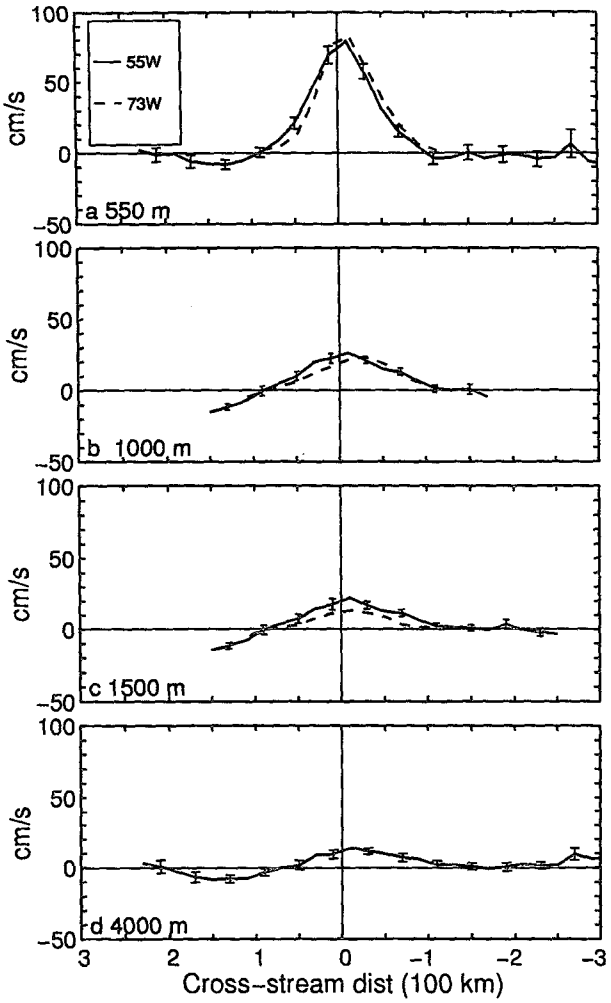

FIG. 17. Mean downstream velocity at 73°W (dashed) and 55°W (solid) at (a) 550 m; (b) 1000 m; (c) 1500 m; and (d) 4000 m, with 95% confidence intervals for 55°W.

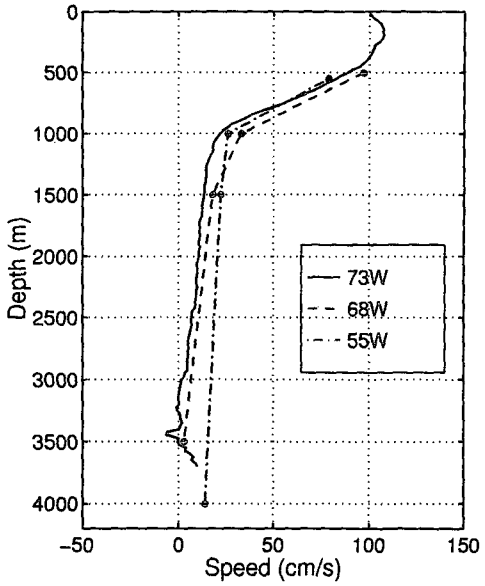

FIG. 18. Vertical profiles of mean downstream velocity from near the center of the jet at 73°W (solid line), 68°W (dashed), and 55°W (dash–dotted).

float observations and thus is probably not as accurate as what we have calculated with the current meter data.

At 1000 m, the two velocity profiles are similar but with the 73°W profile offset somewhat to the south. At the deepest common level, 1500 m, the downstream velocity at 55°W is significantly larger than that at 73°W all across the jet.

To illustrate the change in vertical structure, vertical profiles of downstream velocity near the center of the jet at each location are superimposed in Fig. 18. The most striking difference is the decrease in the vertical shear between the thermocline and abyssal levels at 55°W, caused mostly by a substantial increase in the mean flow in the deep water. At 3500 m, the downstream velocity is only 0–3 cm s^{-1} at the upstream locations and about 15 cm s^{-1} at 55°W. The average synoptic Gulf Stream at 55°W has a much larger barotropic component than at locations upstream of the New England Seamount Chain, but since the total velocity at the thermocline is comparable, the baroclinic component at 55°W is weaker. If we consider the Gulf Stream as a two-layer system, where the thermocline represents the interface between the layers, such a reduction in the baroclinic component should be reflected in the slope of the thermocline. Figure 19 shows the cross-stream distribution of temperature at 550 m at 73° (solid) and 55°W (dashed). The weaker cross-stream gradient at 55°W is brought about not by a substantial widening of the mean synoptic jet but by a change in

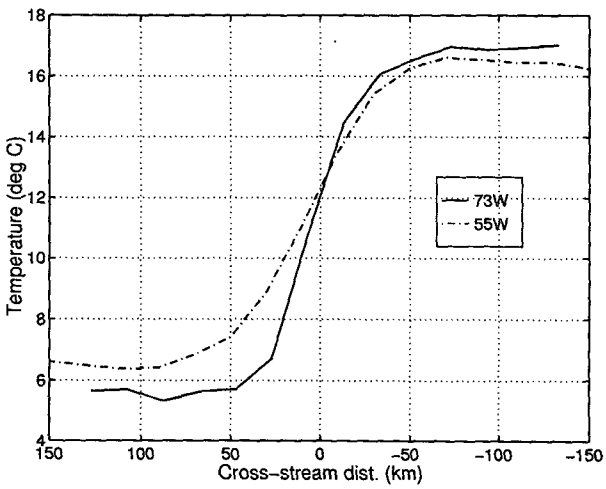

FIG. 19. Cross-stream structure of mean temperature at 73°W (solid) and 55°W (dash–dotted) at 550 m.

the temperature at the edges of the jet, particularly on the north side, where temperature increases by about 1°C in the downstream direction. In order to nullify the effect of this temperature change on density, a salinity increase of about 0.25 psu from west to east would be required on the north side. Maps of the mean salinity north of the Gulf Stream show, however, that salinity *decreases* from west to east, making the cross-stream density gradient even weaker at 55° compared to 73°W than what is indicated from temperature (Worthington 1976; Lozier et al. 1995).

In summary, these results show that the average synoptic Gulf Stream maintains about the same horizontal scale and maximum velocity at the thermocline level between Cape Hatteras and 55°W. The barotropic component increases in magnitude, especially between 68° and 55°W, while the baroclinic component decreases in the downstream direction. The cross-stream velocity structure indicates that there is no significant inflow to or outflow from the Gulf Stream at this longitude. When the shear method was used, a pattern of cross-stream velocity was found that was correlated with meander phase, suggesting that this method may not be suitable for calculating cross-stream flows associated with increasing or decreasing transport.

5. Eddy–mean flow interaction

In the third and final aspect of the structure of the Gulf Stream at 55°W, we consider the interactions between the eddy field and the mean flow in the context of the eddy energy equations. The equation that governs the change in eddy potential energy following the mean flow is derived by multiplying the eddy heat equation by $g\alpha T'/\bar{\theta}_z$ and time averaging. The result is

$$\bar{\mathbf{U}}\cdot\nabla\overline{\mathrm{EPE}} = -\frac{g\alpha}{\bar{\theta}_z}\,\overline{U'T'}\cdot\nabla\bar{T} - g\alpha\overline{w'T'}, \quad (1)$$

where $\mathbf{U}$ is the horizontal velocity vector (u, v), overbars indicate a time mean, primes indicate deviation from the time mean, g is the acceleration due to gravity, α is the effective thermal expansion coefficient, and $\overline{\mathrm{EPE}} = g\alpha\overline{T'T'}/2\bar{\theta}_z$. This equation states that changes in mean EPE following the mean flow are balanced by up- or downgradient heat fluxes (first term on rhs) and the conversion between EPE and EKE (second term on rhs). In the present study, we attempt only a preliminary analysis of this equation by examining the magnitude and distribution of eddy heat flux and its relationship to the mean temperature gradient.

Figures 20a and 20c show the eddy heat flux vectors at 550 and 4000 m with the 95% confidence intervals (boxes), and Figs. 20b and 20d show the heat flux vectors superimposed on the mean temperature field. At 550 m, moorings 1–7 indicate strong eastward eddy heat flux that is statistically significant at moorings 2–5. However, all the heat flux vectors are oriented along, rather than across, the contours of mean temperature (within the uncertainty of the heat flux measurement), suggesting that there is no change in EPE following the mean flow due to up- or downgradient heat fluxes at the thermocline level.

Eddy heat flux at 4000 m is generally eastward in the northern half of the array, although only two estimates are significant (numbers 4 and 5). The similarity of the heat flux pattern at the two depths suggests that in this area on the north side of the jet, the eddies have a relatively barotropic structure. Three sites in the array have a meridional heat flux that is statistically significant (numbers 4, 6, and 13). Mooring 4 is in the strong westward recirculation north of the mean stream at this depth (see Fig. 6c). The sense of the flux is upgradient at this location, suggesting that the eddies are giving up energy to the mean flow or that eddy potential energy is decreasing in the direction of the mean flow (westward at this site). This interpretation should be considered more speculative than conclusive since the uncertainty in the mean temperature field is relatively large near the edges of the array.

The upgradient flux at mooring 6 is also interpreted with caution because it is located at the eastern edge of the array. However, it is consistent with a decrease in eddy energy downstream of the array, a feature that shows up in Schmitz's map of abyssal eddy kinetic energy, Fig. 3b.

Perhaps the most robust signal in the 4000-m eddy heat flux is the southward flux at moorings 10, 11, and 13. This pattern supports the conclusion of previous studies that have shown the westward recirculation to be baroclinically unstable (Hogg 1985; McWilliams 1983). It is of interest to note that while there is evidence of instability of the westward recirculation in the heat flux, there is no evidence of mean westward flow in this region at 4000 m, Fig. 6c.

The eddy kinetic energy equation results from taking the scalar product of the perturbation velocity with the eddy momentum equation and time averaging,

$$\begin{aligned}\bar{\mathbf{U}}\cdot\nabla\overline{\mathrm{EKE}} = &-\left(\overline{u'u'}\frac{\partial\bar{u}}{\partial x} + \overline{u'v'}\left(\frac{\partial\bar{u}}{\partial y} + \frac{\partial\bar{v}}{\partial x}\right) + \overline{v'v'}\frac{\partial\bar{v}}{\partial y}\right)\\ &-\frac{\partial}{\partial x}\left(\frac{\overline{u'p'}}{\rho_0}\right) - \frac{\partial}{\partial y}\left(\frac{\overline{v'p'}}{\rho_0}\right)\\ &-\frac{\partial}{\partial z}\left(\frac{\overline{w'p'}}{\rho_0}\right) + g\alpha\overline{w'T'},\end{aligned}$$

where $\overline{\mathrm{EKE}}$ is the mean eddy kinetic energy, $(\overline{u'u'} + \overline{v'v'})/2$. Here we concern ourselves only with the first term on the rhs, traditionally referred to as the barotropic conversion term. It reflects the production (or destruction) of eddy kinetic energy through interactions between the eddies and the horizontal shear of the mean flow. The remaining terms represent the work

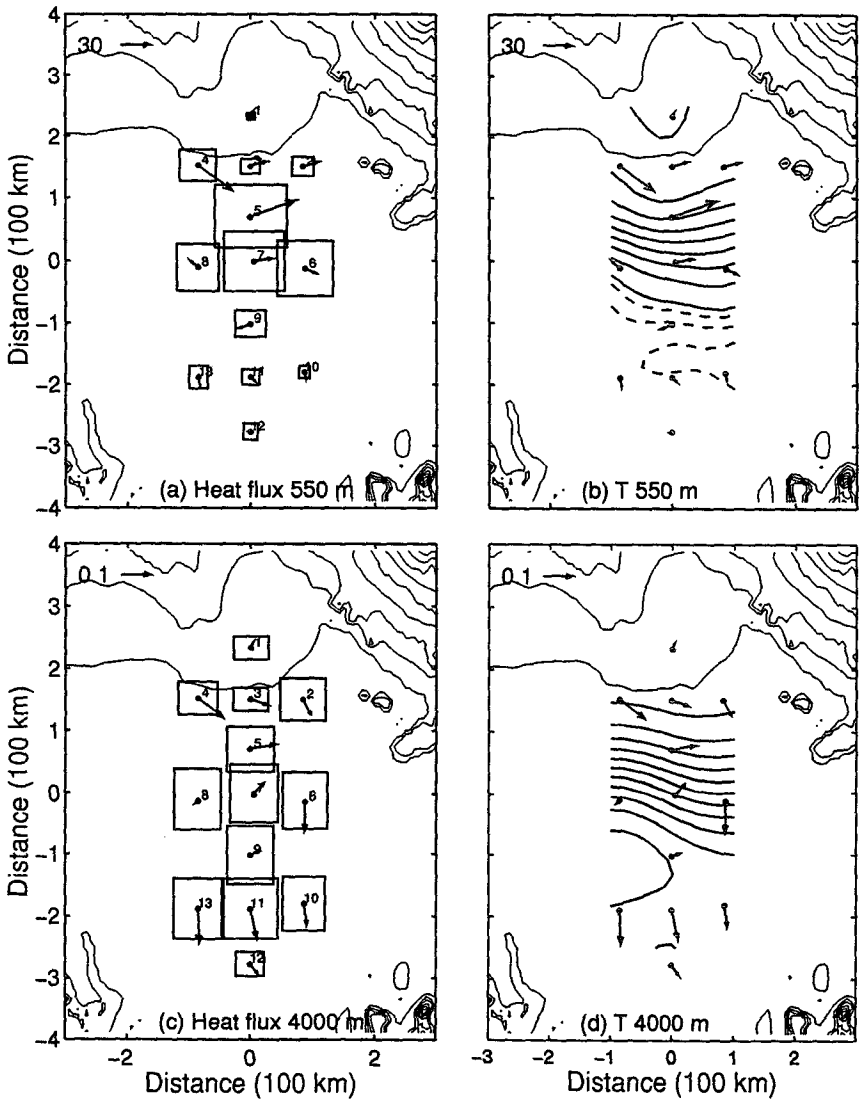

FIG. 20. Mean heat flux vectors with 95% confidence intervals at (a) 550 m and (c) 4000 m. Vectors are superimposed on mean temperature fields in (b) and (d). (Units are cm °C s^{-1}.)

done by the perturbation pressure field and the conversion between eddy potential and eddy kinetic energy.

Consider first the terms involving velocity variance,

$$\overline{u'u'}\,\frac{\partial \bar{u}}{\partial x}$$

and

$$\overline{v'v'}\,\frac{\partial \bar{v}}{\partial y}.$$

While velocity variance is a maximum in the center of the array, the x gradient of eastward velocity along the three zonal lines of moorings and the y gradient of northward velocity along the central north–south line are not significantly different from zero at the 95% confidence level, as seen in Fig. 21a and 21d. Thus, during the SYNOP measurement period, there appears to be no significant contribution to eddy growth or decay via these terms.

This leaves only the term involving the velocity covariance, $\overline{u'v'}$, as a possible contributor to the eddy–mean flow interaction. It is multiplied by the sum of the y-gradient of the zonal velocity (Fig. 21b) and the x gradient of the meridional velocity (Fig. 21c), which *are* significantly different from zero. However, the covariance itself is significant only at one of the mooring sites at 550 m. The generally circular shape of the variance ellipses, Fig. 22a, indicates that there is little correlation between the velocity components. Only moor-

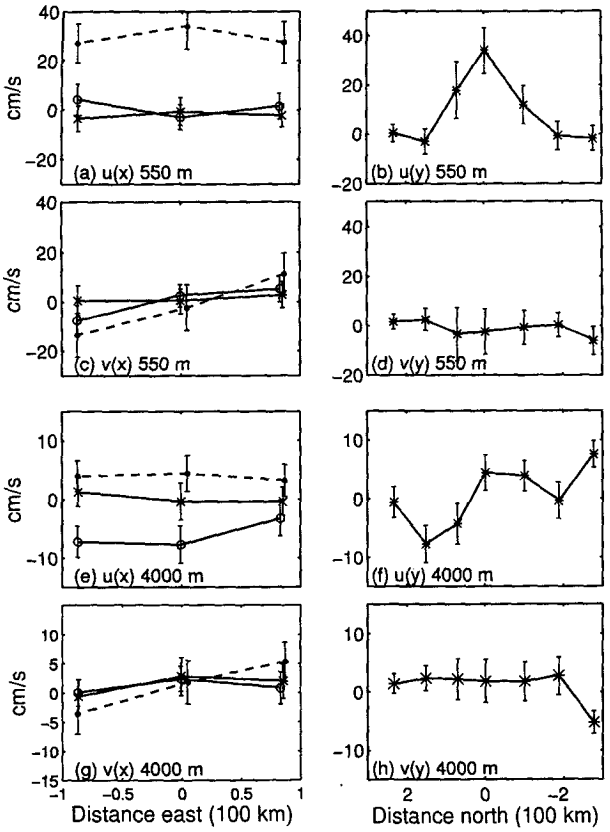

FIG. 21. (a) Distribution of east velocity along three zonal lines of current meters. O: northern line (moorings 2–4), dots and dashes: central line (moorings 6–8), ×: southern line (moorings 10, 11, 13). (b) Distribution of east velocity along central meridional line of moorings (1, 3, 5, 7, 9, 11, and 12). (c) Same as (a) but showing north velocity. (d) Same as (b) but showing north velocity. (e–f) Same as (a–d) but for 4000 m. Ninety-five percent confidence intervals are indicated.

ing 4 has a covariance statistically different from zero at the 95% level, but since it is in a region of weak horizontal shear (see Fig. 6a), this probably does not represent a significant source or sink of EKE. The alignment of the ellipse at mooring 4 at this depth (and at 4000 m, see below) with the bathymetry suggests some influence of the bathymetry in polarizing the eddy motion there.

Essentially the same results were found at 4000 m. The zonal gradients of u and the meridional gradient of v are not distinguishable from zero, Figs. 21e,h. The strong southward velocity observed at the southern end of the central line of moorings is believed to be locally enhanced by the small topographic bump discussed previously. The meridional gradient of zonal velocity *is* significant, Figs. 21f,g, but again most of the covariance estimates are dominated by noise. Only the estimates at moorings 2 and 4 are statistically significant.

In spite of the lack of statistical significance in velocity covariance at this depth, there is a pattern of generally negative values to the north and positive values to the south, Fig. 22b. This pattern is consistent with the radiation of barotropic Rossby waves from the Gulf Stream (Bower and Hogg 1992). To the north, the eddy–mean flow interaction is probably insignificant since the largest Reynolds stress is observed where the horizontal shear of mean velocity is zero (see Fig. 6c). South of the stream axis however, the large positive covariance occurs at mooring 9, where the zonal velocity is increasing northward on the anticyclonic side of the mean jet, which according to Eq. (2) implies a decrease in eddy kinetic energy to the east. This is consistent with the pattern of abyssal EKE observed by Schmitz (1984). But again, the uncertainty in these covariance estimates renders the above interpretation more suggestive than conclusive.

Based on these results, we can summarize the eddy–mean flow interactions at 55°W as follows. At the thermocline level, there is no convincing evidence of significant eddy–mean flow interaction. Cross-gradient heat fluxes are not detectable above the noise, and the Reynolds stresses also cannot be distinguished from zero at 12 of the 13 mooring sites. From this we conclude that at the thermocline level, 55°W is located at the maximum in eddy energy and that the region of decreasing eddy energy, and its associated upgradient fluxes, must lie somewhere between 55°W and the Tail of the Grand Banks at 50°W.

At abyssal levels, there is a suggestion of upgradient eddy heat flux at the eastern edge of the array that might be related to a decrease in eddy energy following the Gulf Stream mean flow to the east. Southward heat flux south of the stream is consistent with baroclinic instability of the westward recirculation, although curiously, the mean flow associated with that recirculation was not detected at this depth. Although not statistically significant, there is a pattern of positive velocity covariance estimates to the south and negative values to the north. The positive values, combined with the anticyclonic shear on the south side of the mean jet, are consistent with a decrease in eddy kinetic energy in the downstream direction.

6. Summary

These analyses have provided an updated view of the Gulf Stream and its relationship to the general circulation at 55°W. In the geographic reference frame, the three-dimensional array of current and temperature measurements from the SYNOP Eastern Array reveal a mean Gulf Stream extending from the thermocline level to 4000 m. In the upper water column, the eastward jet dominates the circulation, while at depth, a westward counterflow was found north of the stream that has about the same magnitude as the eastward mean flow (5–10 cm s^{-1}). Little evidence of a southern recirculation was found within the array.

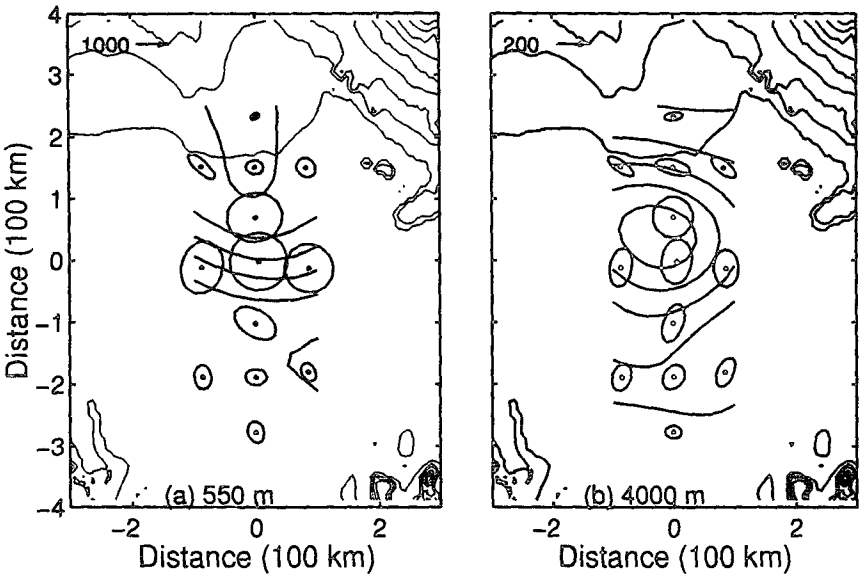

FIG. 22. Variance ellipses for (a) 550- and (b) 4000-m velocity superimposed on mean streamfunction field. (Units are $cm^2\ s^{-2}$.)

In comparing the structure of the mean geographic Gulf Stream during SYNOP with a previous description based on surface drifter, float, and current meter data collected over a seven year time span by Richardson (1985), we found that the jet was narrower, stronger, and more vertically aligned during SYNOP. These differences are probably the result of interannual variability in the mean Gulf Stream path position and meander activity. In particular, the large shift in the velocity maximum with depth (1° latitude) apparent in the Richardson section is probably the result of combining data from different time periods and not a real feature of the mean geographic Gulf Stream. Eddy kinetic energy levels are comparable in both realizations, with values on the order of 1000 $cm^2\ s^{-2}$ in the thermocline and 100 $cm^2\ s^{-2}$ at depth. The SYNOP data were combined with the POLYMODE current meter data to reexamine the total transport across 55°W between 33°–42°N, and it was found that the range of values, 3 ± 35 Sv to 49 ± 41 Sv, is consistent with what is expected from Sverdrup dynamics, about 10 Sv.

The velocity data from the Eastern Array were transformed into a streamwise coordinate system and compared to similar descriptions from upstream locations (73° and 68°W) to examine changes in the Gulf Stream's average synoptic structure. The following summarizes the most salient points concerning the downstream velocity structure. First, at the thermocline level, the Gulf Stream has the same width and peak velocities at all three locations, despite the large amplitude meanders that develop in this region. Second, the barotropic component of downstream velocity increases by about a factor of five: the mean flow at 3500 m increases from 3 cm s^{-1} at 68°W to 15 cm s^{-1} at 55°W. This is accompanied by a weakening of the baroclinic component, which is also evident in the cross-stream temperature gradient. This change in the vertical structure of downstream velocity could be the result of baroclinic instability in the region upstream of 55°W, which would act to lower the available potential energy and enhance the barotropic velocity component.

The cross-stream velocity structure is noisier than that found at the two upstream locations. A detailed analysis of the relationship between cross-stream velocity and flow direction showed that when the shear method is used, there is a pattern of cross-stream velocity associated with meanders similar to what has been observed in the Gulf Stream at other locations. It is concluded that the shear method is not appropriate for observing flows into or out of the stream that are associated with transport changes. The mapping method, which provides a more accurate measure of these flows, indicates that there is no substantial inflow to or outflow from the Gulf Stream at 55°W. This is consistent with there being an elongated maximum in Gulf Stream transport between 60° and 55°W as found by Hogg (1992).

Finally, a preliminary examination of eddy–mean flow interaction at 55°W through the eddy energy equations indicated that at the thermocline level there is no detectable energy transformation between the eddies and the mean flow. No crossgradient eddy heat or momentum fluxes were detected above the noise. At the abyssal level, there was some evidence of upgradient

eddy heat and momentum fluxes at a few sites that would be consistent with decreasing eddy energy in the downstream direction.

New observations of ocean circulation improve our description and, ultimately, our understanding of the dynamics that govern its variability. But they also point toward new questions that, if answered, would lead to yet a more complete view of the circulation. Based on what has been shown here and in Hogg (1992), the Gulf Stream at 55°W is a coherent, energetic current with an average synoptic structure at the thermocline level similar to what is found upstream. Transport and eddy energy appear to be near maximum levels. Between 55°W and the Tail of the Grand Banks, a distance of only about 400 km, significant changes probably occur in the Gulf Stream. The Southeast Newfoundland Rise imposes a strong bathymetric control, which is absent at 55°W, and mean potential vorticity contours for the deep water imply a large decrease in transport on the north side of the Stream (Hogg and Stommel 1985). The true decay region of the Gulf Stream, where eddy energy and transport finally decrease, is probably located in this short stretch of ocean.

Acknowledgments. This work was supported by the U.S. Office of Naval Research under Grants N00014-93-1-0410 and N00014-85-C-0001, NR 083-884, and by the National Science Foundation through Grant OCE86-08258. The authors are grateful to W. Johns, R. Pickart, and the reviewers for their thoughtful comments.

REFERENCES

Bower, A. S., and N. G. Hogg, 1992: Evidence for barotropic wave radiation from the Gulf Stream. *J. Phys. Oceanogr.*, **22,** 42–61.

Bretherton, F. P., R. Davis, and C. Fandry, 1976: A technique for objective analysis and design of oceanographic experiments. *Deep-Sea Res.*, **23,** 559–582.

Cronin, M., and D. R. Watts, 1996: Eddy–mean flow interaction in the Gulf Stream at 68°W. Part I: Eddy energetics. *J. Phys. Oceanogr.*, in press.

Daley, R., 1991: *Atmospheric Data Analysis.* Cambridge University Press, 457 pp.

Dewar, W. K., and J. M. Bane, 1989: Gulf Stream dynamics. Part II: Eddy energetics at 73°W. *J. Phys. Oceanogr.*, **19,** 1574–1587.

Halkin, D., and T. Rossby, 1985: The structure and transport of the Gulf Stream at 73°W. *J. Phys. Oceanogr.*, **15,** 1439–1452.

Hall, M. M., 1986: Assessing the energetics and dynamics of the Gulf Stream at 68°W from moored current measurements. *J. Mar. Res.*, **44,** 423–443.

Hallock, Z. R., 1992: Objective daily maps of thermocline depth for the SYNOP Eastern Array. Tech. Note 259, Naval Oceanographic and Atmospheric Research Laboratory, Stennis Space Center, MS, 54 pp.

Hogg, N. G., 1985: Evidence for baroclinic instability in the Gulf Stream recirculation. *Progress in Oceanography,* Vol. 14, Pergamon, 209–229.

——, 1991: Mooring motion corrections revisited. *J. Atmos. Oceanic Technol.*, **8,** 289–295.

——, 1992: On the transport of the Gulf Stream between Cape Hatteras and the Grand Banks. *Deep-Sea Res.*, **39,** 1231–1246.

——, and H. S. Stommel, 1985: On the relation between the deep circulation and the Gulf Stream. *Deep-Sea Res.*, **32,** 1181–1193.

——, R. S. Pickart, R. M. Hendry, and W. J. Smethie Jr., 1986: The northern recirculation gyre of the Gulf Stream. *Deep-Sea Res.*, **33,** 1139–1165.

Holland, W. R., and P. B. Rhines, 1980: An example of eddy-induced ocean circulation. *J. Phys. Oceanogr.*, **10,** 1010–1031.

Johns, W. E., T. J. Shay, J. M. Bane, and D. R. Watts, 1995: Gulf Stream structure, transport and recirculation near 68°W. *J. Geophys. Res.*, **100,** 817–838.

Kelly, K. A., 1991: The meandering Gulf Stream as seen by the Geosat altimeter: Surface transport, position, and velocity variance from 73° to 46°W. *J. Geophys. Res.*, **96,** 16 721–16 738.

Leetmaa, A., and A. F. Bunker, 1978: Updated charts of mean annual wind stress, convergences in the Ekman layers, and Sverdrup transports in the North Atlantic. *J. Mar. Res.*, **36,** 311–322.

Lindstrom, S. S., and D. R. Watts, 1994: Vertical motion in the Gulf Stream near 68°W. *J. Phys. Oceanogr.*, **24,** 2321–2333.

Lozier, M. S., and S. P. Riser, 1990: Potential vorticity sources and sinks in a quasigeostrophic ocean: Beyond western boundary currents. *J. Phys. Oceanogr.*, **20,** 1608–1627.

——, W. B. Owens, and R. G. Curry, 1995: The climatology of the North Atlantic. *Progress in Oceanography,* Vol. 36, Pergamon, 1–44.

Marshall, J., and G. Shutts, 1981: A note on rotational and eddy heat fluxes. *J. Phys. Oceanogr.*, **11,** 1677–1680.

McWilliams, J. C., 1983: On the mean dynamical balances of the Gulf Stream Recirculation Zone. *J. Mar. Res.*, **41,** 427–460.

Niiler, P. P., W. J. Schmitz, and D.-K. Lee, 1985: Geostrophic volume transport in high eddy-energy areas of the Kuroshio Extension and Gulf Stream. *J. Phys. Oceanogr.*, **15,** 825–843.

Owens, W. B., and N. G. Hogg, 1980: Oceanic observations of stratified Taylor columns near a bump. *Deep-Sea Res.*, **27,** 1029–1045.

Pickart, R. S., 1992: Space–time variability of the deep western boundary current oxygen core. *J. Phys. Oceanogr.*, **22,** 1047–1061.

Richardson, P. L., 1983: Eddy kinetic energy in the North Atlantic from surface drifters. *J. Geophys. Res.*, **88,** 4355–4367.

——, 1985: Average velocity and transport of the Gulf Stream near 55°W. *J. Mar. Res.*, **43,** 83–111.

Rossby, T., 1987: On the energetics of the Gulf Stream at 73°W. *J. Mar. Res.*, **45,** 59–82.

Schmitz, W. J., 1984: Abyssal eddy kinetic energy in the North Atlantic. *J. Mar. Res.*, **42,** 509–536.

Shaw, P.-T., and T. Rossby, 1984: Toward a Lagrangian description of the Gulf Stream. *J. Phys. Oceanogr.*, **14,** 528–540.

Stommel, H. S., 1965: *The Gulf Stream: A Physical and Dynamical Description.* 2d ed., University of California Press, 248 pp.

Tarbell, S. A., S. E. Worrilow, and N. G. Hogg, 1992: A compilation of moored current meter data from SYNOP Arrays One and Two (September 1987 to July 1991), Vol. 64, Woods Hole Oceanographic Institution Tech. Rep. WHOI-93-01, 87 pp. + 7 microfiche.

Thompson, J. D., and W. J. Schmitz Jr., 1989: A limited-area model of the Gulf Stream: Design, initial experiments and model–data intercomparison. *J. Phys. Oceanogr.*, **19,** 792–814.

Worthington, L. V., 1976: *On the North Atlantic Circulation. The Johns Hopkins Oceanographic Studies,* No. 6, 110 pp.